Inorganica Chimica Acta, *132* (1987) 111–118

Structural Chemistry and Magnetism of Dicyclopentadienidehalides of Lanthanides. Part 2*. Dysprosium- and Erbium-dicyclopentadienidebromide, $[Dy(C_5H_5)_2Br]_2$ and $[Er(C_5H_5)_2Br]_2$

HEIKO LUEKEN**, WILLI LAMBERTS and PETER HANNIBAL

Institut für Anorganische Chemie der Technischen Hochschule Aachen, Professor-Pirlet-Strasse 1, D-5100 Aachen, F.R.G.

(Received January 28, 1987)

Abstract

The crystal structures of dysprosium- and erbium-dicyclopentadienidebromide, $[Dy(C_5H_5)_2Br]_2$ (**I**) and $[Er(C_5H_5)_2Br]_2$ (**II**), have been determined from X-ray diffraction data. The two compounds crystallize in the $[Sc(C_5H_5)_2Cl]_2$-type structure, space group $P2_1/c$, with $a = 14.049(9)$, $b = 16.422(9)$, $c = 13.704(5)$ Å, $\beta = 93.51(4)°$, $V = 3156(5)$ Å^3, $D_c = 2.352$ g cm^{-3} (for **I**) and $a = 13.993(3)$, $b = 16.363(3)$, $c = 13.688(4)$ Å, $\beta = 93.75(2)°$, $V = 3127(2)$ Å^3, $D_c = 2.404$ g cm^{-3} (for **II**) and $Z = 6$ dimers. The structures have been refined by full matrix least-squares techniques to conventional R factors of 0.048 for 3362 (**I**) and 0.033 for 4318 (**II**) reflections (with $I > 2\sigma(I)$). Magnetic susceptibility data ($3.6 < T < 295$ K) show in the high temperature region Curie–Weiss behaviour and magnetic moments consistent with those expected for trivalent ions. Due to ligand field effects deviations are observed at low temperatures. At 6 K, **I** exhibits a susceptibility maximum which could be caused by antiferromagnetically coupled dysprosium ions within the binuclear species.

Introduction

Compounds of the type $Ln(C_5H_5)_2X$ (Ln = lanthanide, X = halide) appeared to be relevant when investigating magnetic exchange effects between lanthanide ions, as they are assumed to consist of binuclear species [2] similar to those found in the crystal structure of $[Sc(C_5H_5)_2Cl]_2$ [3]. In the case of the dicyclopentadienidebromide of gadolinium, however, structural investigations show that besides a modification with the expected dimers a polymeric structure exists with double chain arrangement of the heavy atoms [1]. We set out to determine the crystal structures of the corresponding dysprosium and erbium compounds and to investigate their magnetic properties.

Experimental

Preparation

All procedures have been carried out under argon which in the last stage was purified by titanium at a temperature of 850 °C. The compounds were prepared by stoichiometric reaction of water-free sublimed $DyBr_3$ and $ErBr_3$ respectively (purity of the starting material $LnBr_3{\cdot}xH_2O$ 99.99%, Johnson-Matthey Company, U.K.) with colourless NaC_5H_5 in benzene, following standard methods [1, 4].

Mass Spectroscopy

$Dy(C_5H_5)_2Br$ and $Er(C_5H_5)_2Br$ were characterized by mass spectroscopy using the double-focusing Varian MAT CH 5 DF mass-spectrometer with electron energies of 70 eV (temperature of the ion source 170 °C). The spectra were consistent with the corresponding investigations on the analogous $Gd(C_5H_5)_2Br$ [1].

Structural Investigations

Weissenberg photographs (Fe Kα and Mo Kα radiation) were used to determine crystal quality, cell constants and systematic absences. Intensities for structure determination were collected by an Enraf–Nonius CAD 4 automatic diffractometer using graphite monochromated Ag Kα radiation ($\lambda = 0.56083$ Å; ω–2θ scan) at room temperature. Lattice parameters were determined by least-squares refinements of the setting angle of 25 computer-centered reflections in the range $5° < \theta < 15°$. Three standard reflections were monitored every 150 reflections to check crystal stability. No decrease of intensity during data collection was observed. Details concerning crystal size, unit cell, density, number of reflections and absorption coefficients of the two compounds are presented in Table I. The calculations were performed on a VAX 11/730 computer (Digital Equipment Corporation) using the SDP plus program system [5]. Scattering factors for neutral atoms were taken from the International Tables for X-ray Crystallography [6]. For full matrix least-squares refinements, reflections with $I > 2\sigma(I)$ were used. The

---

*Part 1: see ref. 1.

**Author to whom correspondence should be addressed.

0020-1693/87/$3.50

TABLE I. Details and Results of Structural and Magnetochemical Investigations

Compound	$[Dy(C_5H_5)_2Br]_2$ (I)	$[Er(C_5H_5)_2Br]_2$ (II)
Crystal structure		
Crystal size (mm)	0.33 × 0.25 × 0.28	0.42 × 0.18 × 0.30[a]
θ range	$0.01° \leqslant \theta \leqslant 24°$	$0.01° \leqslant \theta \leqslant 24°$
Space group	$P2_1/c$	$P2_1/c$
a (Å)	14.049(9)	13.993(3)
b (Å)	16.422(9)	16.363(3)
c (Å)	13.704(5)	13.688(4)
β (°)	93.51(4)	93.75(2)
V (Å^3)[c]	3156(5)	3127(2)
Z (dimers)	6	6
D_c (g cm^{-3})	2.352	2.404
Number of reflections	8606	10643
Number of unique reflections	7848	9915
Number of reflections in the refinements	3362	4318
Absorption coefficient μ(cm^{-1})	60.0	65.5
R	0.048	0.033
R_w[b]	0.057	0.041
e.s.d.	1.102	1.020
Major peak in final difference Fourier syntheses (e/Å^3)	1.4	0.8
Magnetism		
Magnetic moment, expt. (Bohr magnetons)	10.6(1)	9.6(1)
Magnetic moment, theor.	10.6	9.58
Paramagnetic Curie temperature (K)	−4.5(5)	−9.5(5)

[a] Empirical absorption correction was applied (PSI-scan, programs PSI and EAC, SDP plus [5]). [b] $w = 1/(\sigma(|F_o|))^2$. [c] The correct volume of the unit cell of $[Gd(C_5H_5)_2Br]_2$ is 3197(2) Å^3 (misprint in part 1 [1]).

positions of the hydrogen atoms were calculated with a C–H bond length of 0.95 Å. In final calculations the H atoms ride on the external bisectors of the C–C–C angles (SDP plus [5]).

Magnetic Susceptibility Measurements

Variable-temperature (3.6–295 K) magnetic susceptibility measurements on powdered samples (weighed portions 0.3–1.2 mg) were carried out on a Faraday balance with $HgCo(SCN)_4$ as standard at low magnetic fields (0.07–0.25 T). Susceptibilities were corrected for the diamagnetism of the molecular system (-190×10^{-11} m^3 mol^{-1}/Ln atom [7], SI units).

Structural Results and Discussion

$[Dy(C_5H_5)_2Br]_2$ (I) and $[Er(C_5H_5)_2Br]_2$ (II) form nearly spherical crystals. The cell parameters (see Table I) resemble those of $[Sc(C_5H_5)_2Cl]_2$ [3] and the three compounds crystallize in the same space group. Therefore, in both cases, the crystal structure of the scandium compound served as a starting model. Specific details concerning the structural refinements (conventional R factor, R_w, weighting scheme, e.s.d., major peaks in final difference Fourier synthesis) are presented in Table I. Atomic parameters are given in Table II, bond distances and bond angles in Table III*. The molecular structure is illustrated in Fig. 1.

Structural refinements confirm the $[Sc(C_5H_5)_2Cl]_2$-type structure for **I** and **II**, *i.e.* including the

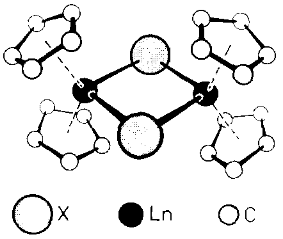

Fig. 1. Molecular structure of $[Ln(C_5H_5)_2X]_2$ (Ln = Dy, Er; X = Br).

---

*See Supplementary Material.

TABLE II. $[Dy(C_5H_5)_2Br]_2$ (I) and $[Er(C_5H_5)_2Br]_2$ (II) Atomic Parameters (all atoms in general position)

Atom	I			II		
	x	*y*	*z*	*x*	*y*	*z*
Ln1	0.04904(5)	0.73206(5)	0.34546(6)	0.04808(3)	0.73248(3)	0.34709(3)
Ln2	0.25889(5)	0.90123(4)	0.44431(5)	0.25748(3)	0.90112(2)	0.44384(3)
Ln3	0.41193(5)	0.40638(4)	0.43737(5)	0.41216(3)	0.40723(2)	0.43710(3)
Br1	0.2111(1)	0.8109(1)	0.2712(1)	0.20906(7)	0.81056(7)	0.27248(7)
Br2	0.0950(1)	0.8267(1)	0.5173(1)	0.09458(8)	0.82748(7)	0.51696(7)
Br3	0.4127(1)	0.5786(1)	0.4503(2)	0.58689(7)	0.42155(6)	0.54843(8)
C1	−0.0431(13)	0.8121(14)	0.2094(16)	−0.0448(9)	0.8103(8)	0.2074(10)
C2	−0.0689(15)	0.8510(12)	0.2960(18)	−0.0639(9)	0.8511(6)	0.2935(11)
C3	−0.1210(13)	0.7965(13)	0.3456(16)	−0.1197(8)	0.7989(8)	0.3462(9)
C4	−0.1326(12)	0.7300(13)	0.2909(15)	−0.1322(8)	0.7300(7)	0.2916(9)
C5	−0.0854(13)	0.7377(14)	0.2085(15)	−0.0871(8)	0.7364(8)	0.2112(9)
C6	0.0098(15)	0.5779(13)	0.3578(16)	0.0093(10)	0.5777(6)	0.3553(10)
C7	0.0471(19)	0.5981(11)	0.4461(17)	0.0426(12)	0.5986(6)	0.4477(10)
C8	0.1390(16)	0.6138(12)	0.4390(21)	0.1395(11)	0.6166(7)	0.4435(12)
C9	0.1608(20)	0.6053(13)	0.3508(20)	0.1616(10)	0.6057(7)	0.3515(12)
C10	0.0822(21)	0.5816(13)	0.2954(19)	0.0804(11)	0.5851(7)	0.2956(11)
C11	0.3491(12)	0.7850(10)	0.5428(14)	0.3467(8)	0.7859(6)	0.5435(9)
C12	0.3994(11)	0.7982(11)	0.4597(14)	0.3976(8)	0.7990(6)	0.4613(8)
C13	0.4417(12)	0.8739(11)	0.4700(13)	0.4400(7)	0.8734(7)	0.4690(8)
C14	0.4167(11)	0.9101(11)	0.5586(14)	0.4127(7)	0.9105(6)	0.5558(8)
C15	0.3573(13)	0.8547(12)	0.6019(11)	0.3561(8)	0.8533(7)	0.6020(8)
C16	0.1484(16)	1.0222(13)	0.3899(19)	0.1474(11)	1.0160(8)	0.3780(14)
C17	0.1683(22)	1.0364(12)	0.4776(19)	0.1648(13)	1.0338(8)	0.4672(13)
C18	0.2590(20)	1.0579(13)	0.4766(20)	0.2590(13)	1.0550(7)	0.4809(11)
C19	0.2963(15)	1.0514(11)	0.3941(19)	0.2992(9)	1.0488(7)	0.3941(12)
C20	0.2185(23)	1.0253(12)	0.3295(18)	0.2286(13)	1.0257(7)	0.3307(10)
C21	0.3697(17)	0.3433(16)	0.2662(14)	0.3704(10)	0.3445(9)	0.2682(8)
C22	0.3817(16)	0.4212(14)	0.2486(13)	0.3829(11)	0.4263(8)	0.2501(8)
C23	0.4768(19)	0.4392(15)	0.2661(12)	0.4779(11)	0.4419(10)	0.2671(8)
C24	0.5238(18)	0.3716(18)	0.2932(14)	0.5208(11)	0.3734(10)	0.2970(8)
C25	0.4581(19)	0.3104(14)	0.2945(16)	0.4609(13)	0.3109(8)	0.2966(9)
C26	0.2724(14)	0.3112(14)	0.4743(16)	0.2774(10)	0.3091(9)	0.4764(11)
C27	0.3423(14)	0.2988(12)	0.5525(17)	0.3426(9)	0.3004(8)	0.5521(9)
C28	0.3433(13)	0.3715(16)	0.6055(14)	0.3455(9)	0.3709(9)	0.6039(8)
C29	0.2783(16)	0.4225(14)	0.5613(16)	0.2814(10)	0.4230(8)	0.5592(10)
C30	0.2380(16)	0.3838(18)	0.4842(21)	0.2397(9)	0.3830(10)	0.4820(11)
H1	−0.0051	0.8347	0.1611	−0.0087	0.8306	0.1563
H2	−0.0521	0.9047	0.3162	−0.0431	0.9044	0.3126
H3	−0.1444	0.8058	0.4082	−0.1444	0.8093	0.4081
H4	−0.1691	0.6838	0.3070	−0.1682	0.6838	0.3096
H5	−0.0807	0.6982	0.1584	−0.0849	0.6952	0.1625
H6	−0.0548	0.5645	0.3404	−0.0544	0.5612	0.3378
H7	0.0124	0.6004	0.5034	0.0070	0.6000	0.5045
H8	0.1816	0.6282	0.4928	0.1823	0.6336	0.4963
H9	0.2219	0.6154	0.3272	0.2235	0.6114	0.3278
H10	0.0791	0.5690	0.2276	0.0750	0.5772	0.2267
H11	0.3149	0.7370	0.5569	0.3113	0.7381	0.5566
H12	0.4032	0.7622	0.4058	0.4023	0.7622	0.4082
H13	0.4825	0.8975	0.4250	0.4811	0.8966	0.4239
H14	0.4369	0.9616	0.5836	0.4295	0.9639	0.5783
H15	0.3269	0.8634	0.6611	0.3290	0.8604	0.6633
H16	0.0864	1.0073	0.3644	0.0884	0.9979	0.3470
H17	0.1256	1.0332	0.5286	0.1185	1.0325	0.5150
H18	0.2909	1.0761	0.5358	0.2901	1.0709	0.5417
H19	0.3614	1.0615	0.3824	0.3642	1.0592	0.3822

(continued)

TABLE II. *(continued)*

Atom	I			II		
	x	*y*	*z*	*x*	*y*	*z*
H20	0.2203	1.0152	0.2613	0.2352	1.0178	0.2627
H21	0.3118	0.3133	0.2623	0.3116	0.3153	0.2630
H22	0.3326	0.4582	0.2280	0.3342	0.4643	0.2300
H23	0.5035	0.4919	0.2592	0.5083	0.4931	0.2586
H24	0.5904	0.3682	0.3098	0.5871	0.3700	0.3169
H25	0.4723	0.2550	0.3090	0.4760	0.2555	0.3114
H26	0.2547	0.2721	0.4255	0.2625	0.2671	0.4275
H27	0.3797	0.2516	0.5663	0.3796	0.2529	0.5675
H28	0.3839	0.3842	0.6621	0.3855	0.3815	0.6610
H29	0.2637	0.4765	0.5804	0.2675	0.4775	0.5775
H30	0.1895	0.4053	0.4403	0.1904	0.4033	0.4378

TABLE III. $[Dy(C_5H_5)_2Br]_2$ (I) and $[Er(C_5H_5)_2Br]_2$ (II) Bond Distances (Å) and Angles (°)[a]

Atoms	I	II
Ln1–Ln2	4.214(1)	4.177(1)
Ln3–Ln3*	4.243(1)	4.204(1)
Br1–Br2	3.844(3)	3.814(2)
Br3–Br3*	3.759(2)	3.720(1)
Ln1–Br1	2.861(2)	2.837(1)
Ln1–Br2	2.862(2)	2.837(1)
Ln2–Br1	2.843(2)	2.819(1)
Ln2–Br2	2.843(2)	2.819(1)
Ln3–Br3	2.834(2)	2.805(1)
Ln3–Br3*	2.835(2)	2.809(1)
Br1–Ln1–Br2	84.40(5)	84.45(3)
Br1–Ln2–Br2	85.06(5)	85.11(3)
Ln1–Br1–Ln2	95.27(6)	95.19(3)
Ln1–Br2–Ln2	95.24(6)	95.20(3)
Br3–Ln3–Br3*	83.07(5)	83.02(3)
Ln3–Br3–Ln3*	96.93(5)	96.98(3)
Next but one metal–metal distances		
Ln1–Ln1	6.877(1)	6.868(1)
Ln1–Ln2	6.759(1)	6.778(1)
Ln1–Ln3	7.443(1)	7.415(1)
Ln2–Ln2	7.582(1)	7.585(1)
Ln2–Ln3	6.973(1)	6.964(1)
Ln3–Ln3*	8.563(1)	8.563(1)
Ln1–C1	2.57(2)	2.58(1)
Ln1–C2	2.62(2)	2.57(1)
Ln1–C3	2.61(2)	2.59(1)
Ln1–C4	2.61(2)	2.59(1)
Ln1–C5	2.58(2)	2.57(1)
Ln1–C6	2.60(2)	2.59(1)
Ln1–C7	2.60(2)	2.59(1)
Ln1–C8	2.61(2)	2.60(2)
Ln1–C9	2.60(2)	2.61(1)
Ln1–C10	2.61(2)	2.56(1)
Ln2–C11	2.62(2)	2.60(1)
Ln2–C12	2.60(2)	2.57(1)
Ln2–C13	2.61(2)	2.59(1)
Ln2–C14	2.64(2)	2.58(1)
Ln2–C15	2.61(2)	2.61(1)
Ln2–C16	2.60(2)	2.56(1)
Ln2–C17	2.61(2)	2.56(1)
Ln2–C18	2.61(2)	2.57(1)
Ln2–C19	2.62(2)	2.59(1)
Ln2–C20	2.62(2)	2.58(1)
Ln3–C21	2.60(2)	2.56(1)
Ln3–C22	2.61(2)	2.58(1)
Ln3–C23	2.63(2)	2.62(1)
Ln3–C24	2.66(2)	2.58(1)
Ln3–C25	2.63(2)	2.61(1)
Ln3–C26	2.58(2)	2.56(1)
Ln3–C27	2.60(2)	2.59(1)
Ln3–C28	2.61(2)	2.59(1)
Ln3–C29	2.62(2)	2.57(1)
Ln3–C30	2.59(2)	2.56(1)
C1–C2	1.41(3)	1.40(2)
C2–C3	1.36(3)	1.39(2)
C3–C4	1.33(3)	1.36(2)
C4–C5	1.35(3)	1.31(2)
C5–C1	1.36(3)	1.35(1)
C6–C7	1.33(3)	1.36(2)
C7–C8	1.33(3)	1.39(2)
C8–C9	1.27(4)	1.33(2)
C9–C10	1.36(4)	1.37(2)
C10–C6	1.37(4)	1.33(2)
C11–C12	1.39(3)	1.39(2)
C12–C13	1.38(3)	1.35(2)
C13–C14	1.42(3)	1.41(2)
C14–C15	1.39(3)	1.40(2)
C15–C11	1.40(3)	1.36(2)
C16–C17	1.24(4)	1.26(3)
C17–C18	1.32(4)	1.36(3)
C18–C19	1.28(4)	1.35(2)

(continued)
(continued)

TABLE III. *(continued)*

Atoms	I	II
C19–C20	1.43(4)	1.33(2)
C20–C16	1.33(4)	1.35(2)
C21–C22	1.31(3)	1.38(2)
C22–C23	1.38(3)	1.36(2)
C23–C24	1.33(4)	1.32(2)
C24–C25	1.37(4)	1.32(2)
C25–C21	1.39(4)	1.41(2)
C26–C27	1.42(3)	1.34(2)
C27–C28	1.40(3)	1.34(2)
C28–C29	1.35(3)	1.36(2)
C29–C30	1.33(3)	1.34(2)
C30–C26	1.30(4)	1.32(2)
C5–C1–C2	106(1)	107(1)
C1–C2–C3	107(2)	107(1)
C2–C3–C4	108(2)	106(1)
C3–C4–C5	110(2)	110(1)
C4–C5–C1	108(2)	110(1)
C10–C6–C7	107(2)	109(1)
C6–C7–C8	108(2)	107(1)
C7–C8–C9	110(2)	107(1)
C8–C9–C10	109(2)	109(1)
C9–C10–C6	106(2)	108(1)
C15–C11–C12	108(2)	108(1)
C11–C12–C13	107(2)	109(1)
C12–C13–C14	110(2)	108(1)
C13–C14–C15	106(2)	107(1)
C14–C15–C11	109(2)	108(1)
C20–C16–C17	118(2)	109(2)
C16–C17–C18	102(3)	108(2)
C17–C18–C19	116(2)	108(1)
C18–C19–C20	104(2)	105(1)
C19–C20–C16	101(2)	109(1)
C25–C21–C22	108(2)	108(1)
C21–C22–C23	108(2)	107(1)
C22–C23–C24	109(2)	108(1)
C23–C24–C25	107(2)	112(1)
C24–C25–C21	108(2)	105(1)
C30–C26–C27	107(2)	108(1)
C26–C27–C28	105(2)	108(1)
C27–C28–C29	108(2)	108(1)
C28–C29–C30	108(2)	106(1)
C29–C30–C26	112(2)	110(1)

[a] Asterisk = symmetry related position.

TABLE IV. Results of Idealization Processes for $[Ln(C_5H_5)_2Br]_2$ (Ln = Gd, Dy, Er)

Unit	Point symmetry	Mean displacements ΔR (Å)		
		Gd	Dy (I)	Er (II)
Dimers				
C_1	D_{2h}	0.03	0.03	0.03
C_i		0.06	0.05	0.04
Metal centres[a]				
Ln1	C_{2v}	0.01	0.02	0.01
Ln2		0.03	0.03	0.03
Ln3		0.06	0.05	0.04
Ln1	D_{2d}, T_d	0.57	0.57	0.56
Ln2		0.58	0.57	0.57
Ln3		0.60	0.60	0.60

[a] With regard to coordinated Br and C_5H_5 (represented by their centre of gravity).

result of part 1 [1] the three dicyclopentadienide-bromides of gadolinium, dysprosium and erbium have the same structure.

With regard to the interpretation of magnetism it is necessary to analyse the symmetry and pseudosymmetry of the metal centres. In the unit cell there are six dimers of which four lie in general position and two on a centre of symmetry. As already mentioned in the discussion of compounds with $[Sc(C_5H_5)_2Cl]_2$-type structure [1, 3], geometrical differences between these two types of dimers are small. This can be shown by calculating the degree of distortion of the real molecular structure from ideal arrangements using the computer program 'PAINLES' [8]. The deviation from ideal geometries is specified by the mean value ΔR of atom displacements. In order to apply the program to the present problem, each C_5H_5 ligand is represented by a pseudo-atom located in the ring centre of gravity. Using this model every metal atom is surrounded by four 'ligands'.

In a first set of calculations the average displacement ΔR has been determined in order to achieve point symmetry D_{2h} for each of the two types of dimers, and in a second step the coordination polyhedra of the three individual metal centres have been idealized to point symmetries C_{2v}, D_{2d} and T_d. The results show (see Table IV) that because of the small ΔR values the dimers (i) have nearly point symmetry D_{2h}, and (ii) tend to greater similarity with increasing atomic number of the lanthanide. (In the case of the gadolinium compound the molecule in the general position is idealized by displacing the ligands to an average of 0.03 Å and each ligand of the centrosymmetric dimer has to be displaced to an average of 0.06 Å, whereas the corresponding displacements for the erbium compound are 0.03 and 0.04 Å, respectively). Following from D_{2h} pseudosymmetry of the binuclear species, the individual metal centres have nearly point symmetry C_{2v}. The deviation from cubic symmetry on the other hand is rather large (ΔR $[T_d]$ = 0.60 Å) which is mainly caused by the widely differing real metal–ligand distances (Ln–Br, Ln–A; A = ring centre of gravity of the coordinated cyclopentadienides).

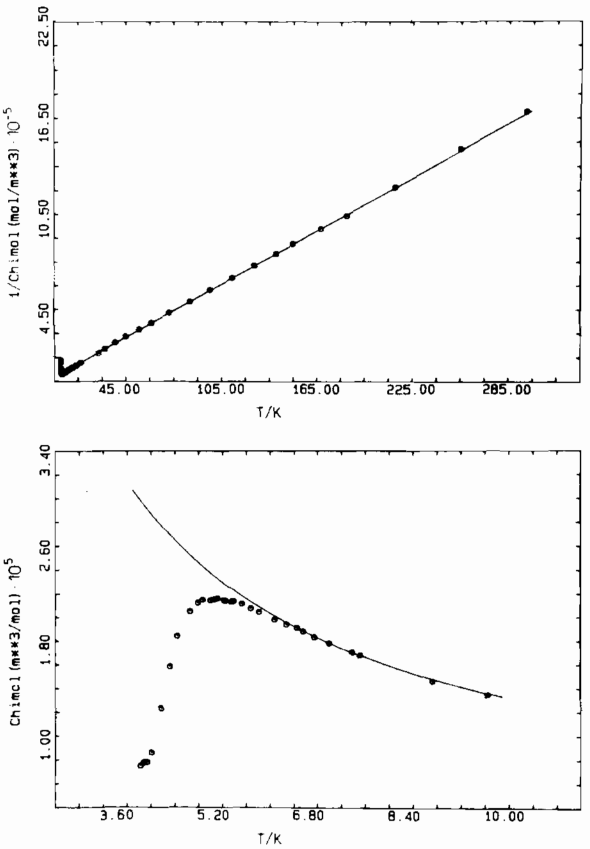

Fig. 2. $[Dy(C_5H_5)_2Br]_2$; $1/\chi_{mol}$ *vs.* T diagram (top) and χ_{mol} *vs.* T. diagram (bottom); ●●●, experimental data; ——, best fit.

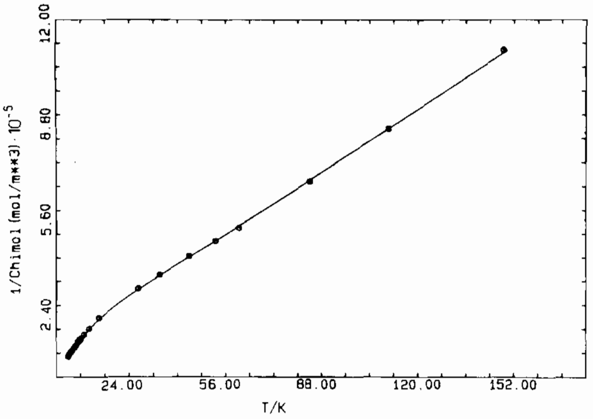

Fig. 3. $[Er(C_5H_5)_2Br]_2$; $1/\chi_{mol}$ *vs.* T diagram; ●●●, experimental data; ——, best fit.

Magnetochemical Investigations

The $1/\chi_{mol}$ *versus* T diagrams of Figs. 2 and 3 show the results of susceptibility measurements and fitting procedures. **I** has a susceptibility maximum at low temperatures and therefore, in analogy with corresponding representations for transition metal complexes, an additional χ_{mol} *vs.* T diagram is chosen (Fig. 2, bottom).

Both compounds show Curie–Weiss behaviour, $\chi_{mol} = C/(T - \theta)$ at high temperatures with a small negative θ value; furthermore the magnetic moments are in agreement with the calculated moments for the free Ln^{3+} ions (see Table I). At low temperatures deviations from the Curie–Weiss straight line occur, the main causes of which may be ligand field effects and interactions between the two paramagnetic centres. In a first approach we have tried to interpret the susceptibility data in terms of a crystal field model as well as a simple molecular field description for magnetic exchange effects, knowing that the susceptibility maximum of **I** at 6 K cannot be reproduced by this approach.

Ligand Field and Molecular Field Model

All lanthanide centres have low point symmetries (C_1 and C_i, respectively). At this level to consider the perturbing influence of the coordinating ligands would be rather cumbersome. To simplify the calculations, the coordination polyhedra of the metal ions have to be idealized with respect to symmetry. From the idealization procedures described above it is obvious that the three different Ln ions (i) can be handled as identical species, and (ii) have pseudosymmetry C_{2v}. The susceptibility data, on the other hand, are obtained from polycrystalline samples, *i.e.* even an orthorhombic ligand field model would still contain more parameters than can be determined from powder data. Therefore the higher symmetries D_{2d} or T_d have to be taken into account. These symmetries, however, can only be achieved: (i) through representing the C_5H_5 rings by pseudoatoms; (ii) by much wider displacements of the 'ligands' than in the case of C_{2v} (see Table IV); and (iii) by neglecting differences in the perturbing influence of the pseudoligands and bromine. Idealization procedures also show that from geometrical arguments differences between D_{2d} and T_d are negligible. Consequently it is convenient to take T_d instead of D_{2d}.

The assumption of lanthanide centres with tetrahedral symmetry in dicyclopentadienidehalide dimers of lanthanides constitutes a drastic approximation. Nevertheless this model can serve as a first attempt (i) to delineate the ligand field effects on the 4f electrons, and (ii) to elucidate the basic differences in magnetic behaviour of the dysprosium and erbium dimers at low temperatures. The terms $^6H_{15/2}$ and $^4I_{15/2}$ of the free ions $Dy^{3+}(4f^9)$ and $Er^{3+}(4f^{11})$, respectively, are used as bases. The influence of a cubic ligand field can be taken into account by applying the Hamiltonian

$$\hat{\mathcal{H}}_{CF} = B_4(\hat{O}_4^0 + 5\hat{O}_4^4) + B_6(\hat{O}_6^0 - 21\hat{O}_4^4)$$

on the manifold of the angular momentum $J = 15/2$ [9], where $\hat{O}_k^q$ are the operator equivalents and coefficients B_k are crystal field intensity parameters (see ref. 9 for further information). The perturbing influence of the cubic crystal field leads to a splitting of the term $J = 15/2$ in two doublets (Γ_6 and Γ_7) and three quartets ($\Gamma_8^{(1)}$, $\Gamma_8^{(2)}$ and $\Gamma_8^{(3)}$). The susceptibility can be calculated from the Van Vleck equation [10]

$$\chi_{\mathrm{CF}} = -\frac{N}{H}\,\frac{\Sigma i(\delta E_i/\delta H)\exp\{-E_i/(kT)\}}{\Sigma i \exp\{-E_i/(kT)\}}$$

where N is Avogadro's number and $-(\delta E_i/\delta H) = \mu_i$ the magnetic moment of the ith level in the direction of the applied field H. (Since Dy^{3+} and Er^{3+} have the same total angular momentum J the susceptibility formulae for **I** and **II** only differ in the Landé g-factor).

In addition to crystal field effects the magnetic behaviour of the lanthanide ions can be influenced by exchange interactions through the intervening halide ions (superexchange). Using the molecular field description the magnetic susceptibility can be given by [11]

$$\frac{1}{\chi} = \frac{1}{\chi_{\mathrm{CF}}} - \lambda$$

where λ is the molecular field parameter. To begin with, fits were carried out for **II** because the erbium compound exhibits a simpler magnetic behaviour. Agreement with experimental data was achieved over the whole temperature range (see solid line in Fig. 3) with a distinct series of crystal field parameters, in which B_4 rises from -1.0×10^{-3} to 7.0×10^{-3} cm^{-1} and B_6 simultaneously from 3.8×10^{-5} to 4.1×10^{-5} cm^{-1}, which meant that the determination of B_4 and B_6 from susceptibility data was not unequivocal. The reason is that in the said series the three lower levels Γ_7, $\Gamma_8^{(1)}$ and Γ_6 shift downwards in energy, whereas the two upper levels $\Gamma_8^{(2)}$ and $\Gamma_8^{(3)}$ shift upwards to nearly the same extent leading to the same susceptibility data. Because of this ambiguity and the applied simple model, a further discussion of the ligand field parameters is meaningless. Some aspects, however, should be mentioned: (i) in the series a doublet lies lowest as predicted for a tetrahedral environment in the case of erbium [9]; (ii) the measured susceptibility data can nearly be explained by ligand field effects alone (the small molecular field parameter $\lambda = -8 \times 10^3$ mol m^{-3} (SI units) corresponds to $\theta = -1$ K in the Curie–Weiss region).

In the case of **I**, satisfactory fits could be achieved over the temperature range $7\ \mathrm{K} < T < 300\ \mathrm{K}$ with B_4 ranging from 5.5×10^{-3} to 8.5×10^{-3} cm^{-1} and B_6 simultaneously from 1.7×10^{-5} to 2.0×10^{-5} cm^{-1}, so that again the ligand field parameters could not be determined unequivocally. (The molecular field parameter was small and varied in the series from -3×10^3 to -1×10^3 mol m^{-3} corresponding to $-0.5\ \mathrm{K} < \theta < -0.2\ \mathrm{K}$). The drastic decrease of the susceptibility below 6 K, however, could not be reproduced by this model nor by any other more realistic ligand field model. Obviously the low temperature behaviour is caused by an intramolecular antiferromagnetic coupling of the dysprosium ions which is not adequately described in the molecular field approach.

Conclusions

Apart from almost negligible differences in interatomic distances, **I** and **II** only differ in the type of paramagnetic centres, *i.e.* in the composition of total angular momentum $J = 15/2$ of the Ln^{3+} ions. Consequently, it is to be supposed that the observed differences in low temperature behaviour correspond to differences in L and S regarding the two types of paramagnetic centres (Dy^{3+}: $L = 5$, $S = 5/2$; Er^{3+}: $L = 6$, $S = 3/2$). In the case of the dysprosium dimer, which contains the lanthanide ion with the higher total spin angular momentum S, a large deviation from the crystal field only susceptibility is observed. To interpret the magnetic behaviour over this temperature range the coupling of the lanthanide spins has to be described by improved models, *i.e.* by the approach of Heisenberg–Dirac–Van Vleck. On the other hand, it has to be confirmed that the crystal structure is stable down to low temperature, since structural changes can also lead to anomalies in the magnetic behaviour.

Supplementary Material

Details of the structural refinements (tables of anisotropic thermal parameters, listings of observed *vs.* calculated structure factors) and susceptibility measurements can be obtained from the authors on request.

Acknowledgements

Financial support by Deutsche Forschungsgemeinschaft and Fonds der Chemischen Industrie is gratefully acknowledged. The authors thank M. Deussen for carefully measured magnetic susceptibilities.

References

1 W. Lamberts, H. Lueken and U. Elsenhans, *Inorg. Chim. Acta, 121,* 81 (1986).
2 H. Schumann, *Angew. Chem., 96,* 475 (1984).
3 J. L. Atwood and K. D. Smith, *J. Chem. Soc., Dalton Trans.,* 2487 (1973).
4 R. E. Maginn, S. Manastyrskij and M. Dubeck, *J. Am. Chem. Soc., 85,* 672 (1963).
5 B. A. Frenz, in H. Schenk and R. Olthof-Hazekamp (eds.), 'Computing in Crystallography', Delft University Press, Delft, 1978.

6 D. T. Cromer and J. T. Waber, 'International Tables for X-ray Crystallography', Vol. IV, Kynoch Press, Birmingham, 1974.

7 A. Weiss and H. Witte, 'Magnetochemie – Grundlagen und Anwendungen', Verlag Chemie, Weinheim, 1973.

8 H. Lueken, U. Elsenhans and U. Stamm, *Acta Crystallog., Sect. A, 43,* 187 (1987).

9 K. R. Lea, M. J. M. Leask and W. P. Wolf, *J. Phys. Chem. Solids, 23,* 1381 (1962).

10 J. H. Van Vleck, 'The Theory of Electric and Magnetic Susceptibilities', Oxford University Press, London, 1932.

11 B. Bleaney, *Proc. R. Soc. London, Ser. A, 276,* 19 (1963).